

## Band engineering of carbon nanotube field-effect transistors via selected area chemical gating

Xiaolei Liu, Zhicheng Luo, Song Han, Tao Tang, Daihua Zhang, and Chongwu Zhou<sup>a)</sup>  
*Department of Electrical Engineering, University of Southern California, Los Angeles, California 90089*

(Received 13 December 2004; accepted 27 April 2005; published online 6 June 2005)

This letter presents an approach to engineer the band structure of carbon nanotube field-effect transistors via selected area chemical gating. By exposing the center part, or the contacts, of nanotube devices to oxidizing or reducing gases, a good control over the threshold voltage and subthreshold swing has been achieved. Our experiments reveal that NO<sub>2</sub> shifts the threshold voltage positively, while NH<sub>3</sub> shifts it negatively for both center-exposed and contact-exposed devices. However, modulations to the subthreshold swing are in opposite directions for center-exposed and contact-exposed devices: NO<sub>2</sub> lowers the subthreshold swing of the contact-exposed devices, but increases that of the center-exposed devices. In contrast, NH<sub>3</sub> reduces the subthreshold swing of the center-exposed devices, but increases that of the contact-exposed devices. © 2005 American Institute of Physics. [DOI: 10.1063/1.1944898]

As individual molecular wires, single-walled carbon nanotubes (SWNTs) are intriguing one-dimensional conductors with fascinating transport properties. The lack of traps and scattering centers allows carriers to ballistically transport through the carbon nanotubes with mean free path on the order of a micrometer, which makes carbon nanotubes (CNTs) an excellent candidate material for high performance field-effect transistors. Since SWNTs field-effect transistors (CNT-FETs) were first reported in 1998,<sup>1</sup> great effort has been devoted to understanding the operation of these transistors<sup>2</sup> and improving their performance.<sup>3–7</sup> A number of elegant experiments have been reported toward this goal: For example, metals with a high work function and good adhesion to CNTs were demonstrated to form ohmic contacts;<sup>5</sup> materials with high dielectric constants,<sup>3</sup> and liquid/polymer electrolytes have been used to enhance the gate effect;<sup>4,6,7</sup> and nonuniform electrical doping using split gates has been employed to tailor the band structure of the CNT-FETs.<sup>8</sup> In this letter, we present an interesting approach of using selected area chemical gating to tune the electrical properties of nanotube transistors.

The CNT-FETs are very sensitive to the ambient environment,<sup>9</sup> which makes them very good chemical and biological sensors.<sup>10,11</sup> The electrons or holes can be transferred from the adsorbed molecules, and thus the Fermi level of the exposed CNTs can be shifted. Early work on controlling the CNT-FET characteristics focused on the attachment of oxidizing and reducing chemicals, such as potassium and bromine, to the nanotubes to modulate the Fermi level.<sup>12,13</sup> Later on, nonuniform chemical doping on CNTs was performed to create intramolecular *p-n* junctions.<sup>14</sup> These studies represented significant advances; however, an important parameter widely used to characterize transistor performance, the subthreshold swing, received only limited attention at that time. Using nonuniform doping to control both the threshold voltage and the subthreshold swing of nanotube transistors has not been demonstrated so far. We report, for the first time, that selected-area chemical gating can be em-

ployed to tune the contact transparency relative to the bulk nanotube, which leads to an intriguing influence on both the threshold voltage and the subthreshold swing for the nanotube transistors. This device design can also be used for chemical sensing application, though two-terminal devices may work sufficiently well.<sup>15</sup>

Our CNT-FET devices were fabricated using chemical vapor deposition (CVD) grown SWNTs on silicon substrates covered with 500 nm thermal oxide as the gate dielectric layer.<sup>16</sup> Metallic contacts consisted of 3 nm titanium capped with 60 nm gold, which should form Schottky contacts with the 4 μm long CNTs.<sup>2</sup> Devices showing typical *p*-type transistor characteristics were chosen for further studies. The typical subthreshold swing of these devices measured in ambient environment is 600–800 mV/dec.

In order to modulate the energy band nonuniformly along the nanotubes, poly(methyl methacrylate) (PMMA) was spun on to cover and protect the devices. We verified that the diffusion of gases (NO<sub>2</sub> or NH<sub>3</sub>) through the PMMA layer was negligible, as devices fully covered with PMMA exhibited no response upon chemical exposure. An electron-beam lithography technique was then used to open ~1 μm wide windows in the center or on the contacts of the CNT-FET devices. Figure 1 shows two schematic diagrams for a contact-exposed device and a center-exposed device. Following the electron-beam lithography, the devices were exposed to diluted NH<sub>3</sub> or NO<sub>2</sub>. To test the performance of the CNT-FET devices, a small constant source-drain voltage of 50 mV was applied while the transfer characteristics measurements were made. Figure 2(a) displays the transfer curves for a contact-exposed device residing in air, and in various concentrations of NO<sub>2</sub> and NH<sub>3</sub>. Similar measurements were also performed for a center-exposed device, with the transfer curves shown in Fig. 2(b). After each chemical exposure, the device was always allowed to recover for 30 min to fully return to the initial state (i.e., device in air) before any subsequent chemical exposure. One can clearly see that for both center-exposed and contact-exposed devices, the threshold voltage shifted negatively upon NH<sub>3</sub> exposure but positively upon NO<sub>2</sub> exposure. This is understandable and consistent

<sup>a)</sup>Electronic mail: chongwuz@usc.edu

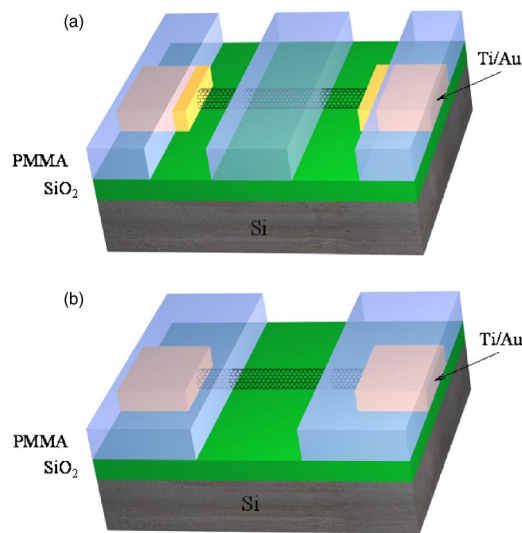


FIG. 1. (Color online) Schematics of the partially exposed CNT transistors used in this study: (a) A contact-exposed device and (b) a center-exposed device.

with pervious experiments,<sup>10</sup> as  $\text{NO}_2$  withdraws electrons from the nanotube and  $\text{NH}_3$  donates electrons to the nanotube. In addition to the shift of the threshold voltage, the subthreshold swing, which is manifested by the slope of the current-voltage ( $I$ - $V_g$ ) curves in the subthreshold region shown in Fig. 2, also changed with respect to the exposure to  $\text{NH}_3/\text{NO}_2$  for our partially exposed devices. In Fig. 2(a), for the contact-exposed nanotube transistor, the subthreshold swing decreased when the device was exposed to  $\text{NO}_2$ , but increased when exposed to  $\text{NH}_3$ . On the contrary, the trend of the subthreshold swing change was reversed for the center-exposed devices as shown in Fig. 2(b): The subthreshold swing became larger when the device was exposed to  $\text{NO}_2$ , but it became smaller when  $\text{NH}_3$  was applied instead.

Qualitatively speaking, for the contact-exposed CNT-FET devices, the  $\text{NO}_2$  molecules adsorbed onto the CNTs donate holes to the CNT-FET devices, and move the valence band of the exposed nanotube part upward relative to the Fermi level. As shown in the schematics in Fig. 2(c), this upward shift of the valence band at contacts makes the Schottky barriers thinner and more transparent for hole injection from the metal electrodes. The overall device charac-

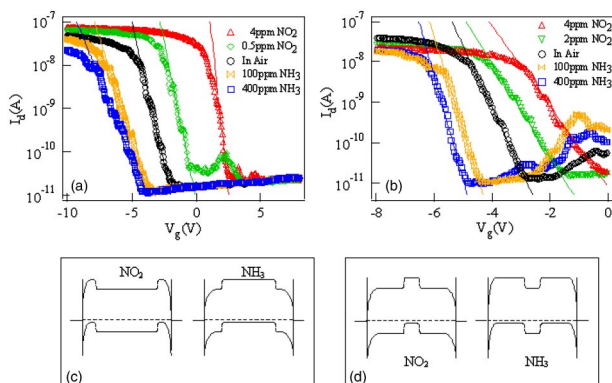


FIG. 2. (Color online)  $I_d$ - $V_g$  curves of a contact-exposed device (a) and a center-exposed device (b) under various ambient conditions. The solid lines are linear fits for the subthreshold regime. (c) and (d) Band structures of the contact-exposed and the center-exposed devices in  $\text{NO}_2$  and  $\text{NH}_3$  at the threshold voltage, respectively.

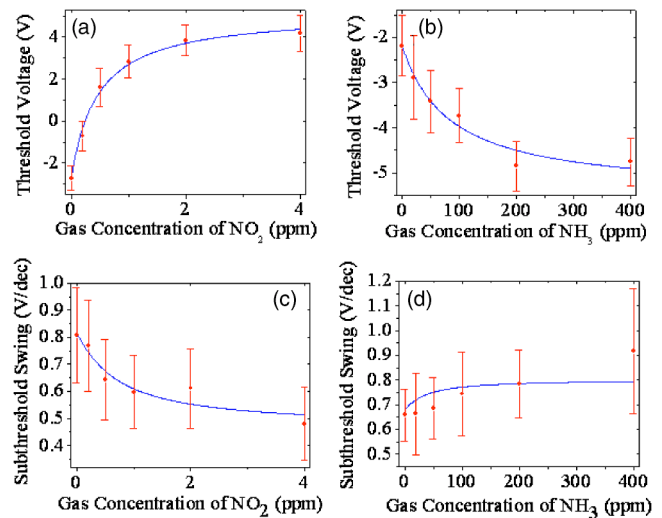


FIG. 3. (Color online) Characteristics of the contact-exposed device (1  $\mu\text{m}$  wide window opened at contacts). (a) and (b) Threshold voltages plotted as functions of  $\text{NO}_2$  and  $\text{NH}_3$  concentrations, respectively. (c) and (d) Subthreshold swings plotted as functions of  $\text{NO}_2$  and  $\text{NH}_3$  concentrations. The solid lines are numerically simulated results.

teristics are then more dominated by the bulk nanotube than by the contacts. Indeed, if doping of the adsorbed  $\text{NO}_2$  molecules is sufficiently high, the CNT segments at contacts may serve as artificial source/drain electrodes to the rest of the nanotube, which behaves more like a metal-oxide-semiconductor (MOSFET) than a Schottky barrier FET (SBFET). The subthreshold swing therefore becomes smaller under  $\text{NO}_2$  exposure for contact-exposed devices, as MOSFETs tend to have a stronger gate dependence and hence a lower subthreshold swing than SBFETs. This is consistent with previous observation,<sup>8</sup> where the energy band modulation at contacts was achieved using a split gate. For the adsorbed  $\text{NH}_3$  molecules, they withdraw holes from the nanotubes and thus make the Schottky barriers thicker and less transparent to the carriers at the threshold voltage. Therefore, a larger subthreshold swing was observed for contact-exposed devices in an  $\text{NH}_3$  ambient.

Similarly, for the center-exposed CNT-FETs, adsorption of  $\text{NO}_2$  shifts the valence band higher relative to the rest part of the nanotube. As shown in Fig. 2(d), the device is now more dominated by the contact barriers and thus gives larger subthreshold swing. However, the adsorbed  $\text{NH}_3$  molecules move the valence band at the center of the nanotube lower. In order to turn on the nanotube, the gate voltage has to bring the valence band of the rest part of the nanotube even higher, therefore leading to a thinner contact barrier, which is more transparent to the carriers. As a result, the subthreshold swing is smaller under this condition.

Furthermore, to obtain quantitative information regarding the dependence of the threshold voltage and subthreshold swing on the gas concentration, the CNT-FET devices were measured under various concentrations for both  $\text{NO}_2$  and  $\text{NH}_3$ . To obtain the stable doping effect under the desired gas concentration, we kept the gas concentration constant and then repeated the transfer characteristic measurements  $\sim 40$  times for every gas concentration. Then, the threshold voltages and subthreshold swings were extracted from the as-measured  $I$ - $V_g$  curves, followed by calculating the mean values and standard deviations, which are shown in Figs. 3 and 4 represented by the data points and error bars.

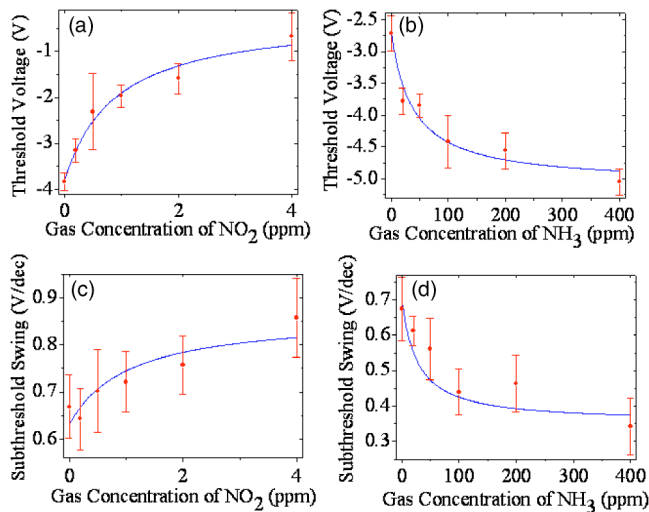


FIG. 4. (Color online) Characteristics of the center-exposed device (1  $\mu\text{m}$  wide window opened in the center). (a) and (b) Threshold voltages plotted as functions of NO<sub>2</sub> and NH<sub>3</sub> concentrations, respectively. (c) and (d) Subthreshold swings plotted as functions of NO<sub>2</sub> and NH<sub>3</sub> concentrations. The solid lines are numerically simulated results.

For the contact-exposed device, the threshold voltage and the subthreshold swing are plotted as functions of gas concentrations in Figs. 3(a) and 3(b). It is apparent that the threshold voltage increased with increasing NO<sub>2</sub> concentration, but decreased with increasing NH<sub>3</sub> concentration. The change to the threshold voltage saturated at high concentrations for both NO<sub>2</sub> and NH<sub>3</sub>. As shown in Figs. 3(c) and 3(d), the mean subthreshold swing decreased from 810 mV/dec to 480 mV/dec with the concentration of NO<sub>2</sub> going up to 4 ppm, while it increased from 660 mV/dec to 920 mV/dec when the NH<sub>3</sub> concentration was increased from 0 to 400 ppm.

For the center-exposed device, the threshold voltage and the subthreshold swing are plotted versus gas concentrations of NO<sub>2</sub> and NH<sub>3</sub> in Figs. 4(a) and 4(b). The threshold voltage variation is similar to that of contact-exposed devices; however, as Figs. 4(c) and 4(d) shows, the mean subthreshold swing increased from 670 mV/dec to 860 mV/dec when the concentration of NO<sub>2</sub> went from 0 to 4 ppm, and decreased from 670 mV/dec to 340 mV/dec when the concentration of NH<sub>3</sub> was increased from 0 to 400 ppm. Our method therefore provides an interesting way to tune both the threshold voltage and the subthreshold swing of nanotube transistors. Further improvement to the subthreshold swing can probably be achieved with a thinner oxide layer and better oxide quality.

There are detailed models<sup>17,18</sup> on the electrical behavior of semiconducting CNTs and the Schottky barrier modulation effect.<sup>8</sup> Here, to analyze the data further, we have included the effect of the Schottky barriers and modeled the threshold voltage shift following the equation:  $\Delta V_T = \pm \frac{kq_nof}{c_g} \theta(p)$ , where  $q$  is the electron charge,  $c_g$  is the gate capacitance for the exposed part of the nanotubes,  $n_0$  is the total number of positions that can be occupied by the adsorbed molecules,  $k$  is a structure parameter characterizing the importance of the exposed part upon the whole device,  $f$  is the charge transfer rate,  $\theta(p)$  is the coverage of the adsorbed molecules as a function of the partial pressure of the gas, and the plus/minus sign depends on whether NO<sub>2</sub> or

NH<sub>3</sub> is used.  $\theta(p)$  can be calculated following the Langmuir adsorption isotherm,<sup>19</sup> and the theoretical results fit the experiments quite well as shown in Figs. 3(a), 3(b), 4(a), and 4(b). To find the subthreshold swing of the selected-area exposed nanotube transistors, we treat the device as serially connected two FETs with different subthreshold swings, one accounting for both contacts and the other for the bulk nanotube. The current of each segment follows  $I_D = I_s e^{-\beta(V_G - V_T)} q V_D / k_B T$  in the subthreshold regime,<sup>20</sup> and the simulated subthreshold swing versus the gas partial pressure is displayed in Figs. 3(c), 3(d), 4(c), and 4(d). The results indicate that a good theoretical guidance can be provided on how to control the nanotube transistor performance with a rational device design and selected-area chemical gating.

In conclusion, selected area chemical gating on nanotube transistors provides an interesting way to design and control the band structure of the devices without the complexity of extra gate electrodes. The goal of gaining control on both the threshold voltage and the subthreshold swing has been achieved by selectively exposing part of the CNT-FETs to reducing and oxidizing gases of different concentrations. Both qualitative and quantitative analyses were given to explain the experiment results theoretically. Our concept of selected area doping can be readily applied to solid-phase doping techniques and render stable nanotube devices mimicking conventional MOSFETs.

The authors gratefully acknowledge financial support from a NSF CAREER Award, a NSF-CENS grant, a Norris Fellowship, and a SRC MARCO/DARPA grant.

- <sup>1</sup>S. J. Tans, A. R. M. Verschueren, and C. Dekker, *Nature (London)* **393**, 49 (1998).
- <sup>2</sup>J. Appenzeller, J. Knoch, V. Derycke, R. Martel, S. Wind, and P. Avouris, *Phys. Rev. Lett.* **89**, 126801 (2002).
- <sup>3</sup>A. Javey, H. Kim, M. Brink, Q. Wang, A. Ural, J. Guo, P. McIntyre, P. McEuen, M. Lundstrom, and H. Dai, *Nat. Mater.* **1**, 241 (2002).
- <sup>4</sup>S. Rosenblatt, Y. Yaish, J. Park, J. Gore, V. Sazonova, and P. L. McEuen, *Nano Lett.* **2**, 869 (2002).
- <sup>5</sup>A. Javey, J. Guo, Q. Wang, M. Lundstrom, and H. J. Dai, *Nature (London)* **424**, 654 (2003).
- <sup>6</sup>C. Lu, Q. Fu, S. Huang, and J. Liu, *Nano Lett.* **4**, 623 (2004).
- <sup>7</sup>S. Huang, M. Woodson, R. Smalley, G. P. Siddons, D. Merchin, J. H. Back, J. K. Jeong, and M. Shim, *Nano Lett.* **4**, 927 (2004).
- <sup>8</sup>S. J. Wind, J. Appenzeller, and P. Avouris, *Phys. Rev. Lett.* **91**, 58301 (2003).
- <sup>9</sup>P. G. Collins, K. Bradley, M. Ishigami, and A. Zettl, *Science* **287**, 1801 (2000).
- <sup>10</sup>J. Kong, N. R. Franklin, C. Zhou, M. G. Chapline, S. Peng, K. Cho, and H. Dai, *Science* **287**, 622 (2000).
- <sup>11</sup>A. Star, J. C. P. Gabriel, K. Bradley, and G. Gruner, *Nano Lett.* **3**, 459 (2003).
- <sup>12</sup>R. S. Lee, H. J. Kim, J. E. Fischer, A. Thess, and R. E. Smalley, *Nature (London)* **388**, 255 (1997).
- <sup>13</sup>J. Kong, C. W. Zhou, E. Yenilmez, and H. J. Dai, *Appl. Phys. Lett.* **77**, 3977 (2000).
- <sup>14</sup>C. W. Zhou, J. Kong, E. Yenilmez, and H. J. Dai, *Science* **290**, 1552 (2000).
- <sup>15</sup>J. Li, Y. Lu, Q. Ye, M. Cinke, J. Han, and M. Meyyapan, *Nano Lett.* **3**, 929 (2003).
- <sup>16</sup>X. Liu, C. Lee, C. Zhou, and J. Han, *Appl. Phys. Lett.* **79**, 3329 (2001).
- <sup>17</sup>T. Yamada, *Appl. Phys. Lett.* **76**, 628 (2000).
- <sup>18</sup>T. Yamada, *Phys. Rev. B* **69**, 125408 (2004).
- <sup>19</sup>P. Qi, O. Vermesh, M. Greco, A. Javey, Q. Wang, H. Dai, S. Peng, and K. J. Cho, *Nano Lett.* **3**, 347 (2003).
- <sup>20</sup>S., M. Sze, *Physics of Semiconductor Devices*, 2nd ed. (Wiley, New York, 1981).